Star Formation News Letter No. 308, #11-20：工藤哲洋

11 **Flux Density Variations at 3.6 cm in the Massive Star-Forming Region W49A**
Christopher De Pree[1], R. Galvn-Madrid[2], W. M. Goss[3], R. S. Klessen[4,5], M.-M. Mac Low[6], T. Peters[7], D. Wilner[8], J. Bates[1], T. Melo[1], B. Presler-Marshal[1] and R. Webb-Forgus[1]

12 **Massive stars in the hinterland of the young cluster, Westerlund 2**
J.E. Drew[1], A. Herrero[2,3], M. Mohr-Smith[1], M. Monguió[1], N.J. Wright[4], T. Kupfer[5,6], R. Napiwotzki[1]

13 **A Molecular Line Investigation of the Interaction between Mid-infrared Bubbles and the Interstellar Medium**
Kathryn Devine[1], Johanna Mori[1], Christer Watson[2], Leonardo Trujillo[1] and Matthew Hicks[2]

14 **Filamentary structures and star formation activities in the sites S234, V582, and IRAS 05231+3512**
Lokesh K. Dewangan[1], Tapas Baug[2], Devendra K. Ojha[3], I. Zinchenko[4] and A. Luna[5]

15 **The Hawaii Infrared Parallax Program. III. 2MASS J0249-0557 c: A Wide Planetary-mass Companion to a Low-mass Binary in the β Pic Moving Group**
Trent J. Dupuy[1], Michael C. Liu[2], Katelyn N. Allers[3], Beth A. Biller[5,6], Kaitlin M. Kratter[7], Andrew W. Mann[8,9], Evgenya L. Shkolnik[10] Adam L. Kraus[11] and William M.J. Best[2]

16 **A WISE Survey of Circumstellar disks in the Upper Scorpius Association**
T.L. Esplin[1,2], K.L. Luhman[3,4], E.B. Miller[3], and E.E. Mamajek[5,6]

17 **First Detection of the Simplest Organic Acid in a Protoplanetary Disk**
Cecile Favre[1], Davide Fedele[1], Dmitry Semenov[2,3], Sergey Parfenov[4], Claudio Codella[1,5], Cecilia Ceccarelli[5], Edwin A. Bergin[6], Edwige Chapillon[7,8], Leonardo Testi[1,9,10], Franck Hersant[7], Bertrand Lefloch[5], Francesco Fontani[1], Geoffrey A. Blake[11], L. Ilsedore Cleeves[12], Chunhua Qi[12], Kamber R. Schwarz[6] and Vianney Taquet[1]

18 **ALMA observations of RCW120 - Fragmentation at 0.01pc scale**
Miguel Figueira[1,2], Leonardo Bronfman[2], Annie Zavagno[1], Fabien Louvet[2], Nadia Lo[2], Ricardo Finger[2] and Javier Rodón[3]

19 **A multi-wavelength view of magnetic flaring from PMS stars**
E. Flaccomio[1], G. Micela[1], S. Sciortino[1], A.M. Cody[2], M.G. Guarcello[1], M. Morales-Calderón[3], L. Rebull[4], and J.R. Stauffer[4]

20 **Depletion of ^{15}N in the center of L1544: Early transition from atomic to molecular nitrogen?**
Kenji Furuya[1], Yoshimasa Watanabe[2,3], Takeshi Sakai[4], Yuri Aikawa[5] and Satoshi Yamamoto[6]

http://arxiv.org/pdf/1807.05768

17

First Detection of the Simplest Organic Acid in a Protoplanetary Disk

Cecile Favre[1], Davide Fedele[1], Dmitry Semenov[2,3], Sergey Parfenov[4], Claudio Codella[1,5], Cecilia Ceccarelli[5], Edwin A. Bergin[6], Edwige Chapillon[7,8], Leonardo Testi[1,9,10], Franck Hersant[7], Bertrand Lefloch[5], Francesco Fontani[1], Geoffrey A. Blake[11], L. Ilsedore Cleeves[12], Chunhua Qi[12], Kamber R. Schwarz[6] and Vianney Taquet[1]

- 原始惑星系円盤で初めてHCOOH（ギ酸）の分子を発見した. （ALMA Cycle3）（星形成領域では発見されていた. ）

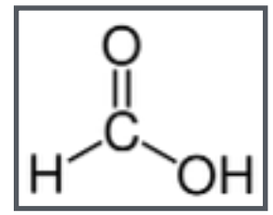

- HCOOHはアミノ酸の主要な要素で, メタノールなどより合成が複雑. 有機化学が活発に起こっている証拠. 生命に関係する複雑な合成が起こっていることを表す.

- TW Hydrae の惑星系円盤. 主星が 0.7 $M_{太陽}$.

円盤からの129 GHz のHCOOH

trans-HCOOH $6_{(1,6)}$–$5_{(1,5)}$ transition

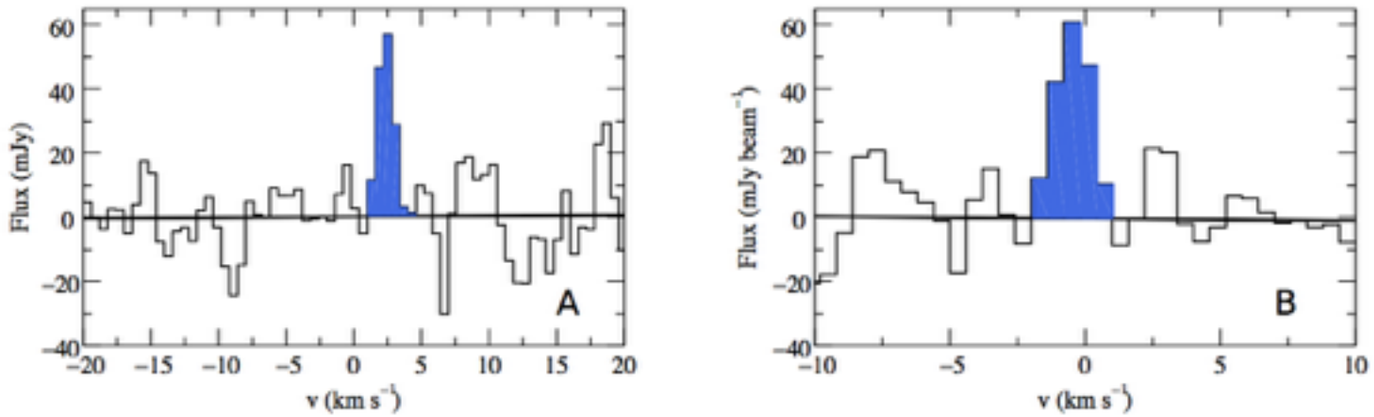

Figure 2. *Panel a*: TW Hya disk-averaged HCOOH spectrum extracted from the original datacube within 400 au . *Panel b*: TW Hya HCOOH spectrum resulting from the pixel spectral stacking method by Yen et al. (2016). The signal to noise ratio is ~5.

HCOOHの柱数密度の推定値

$2 - 4 \times 10^{12}$ cm^{-2}

(methanol と同じくらい)

マップ

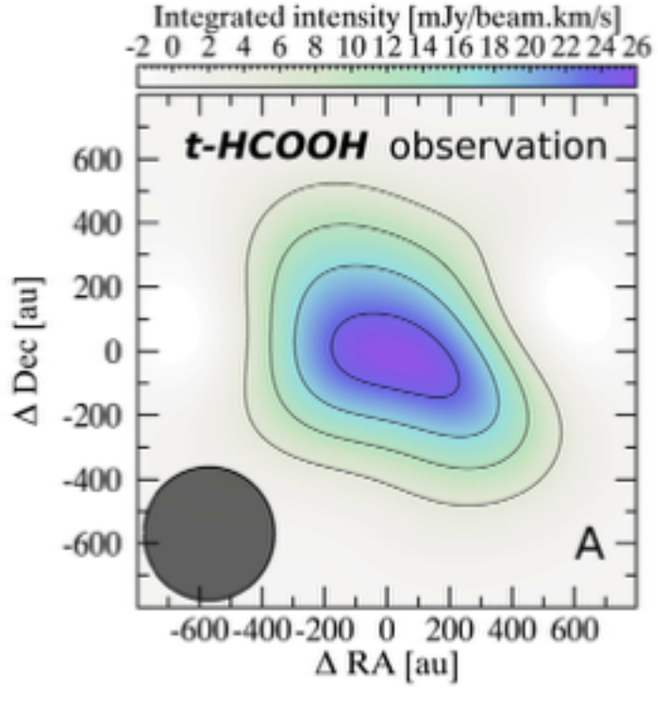

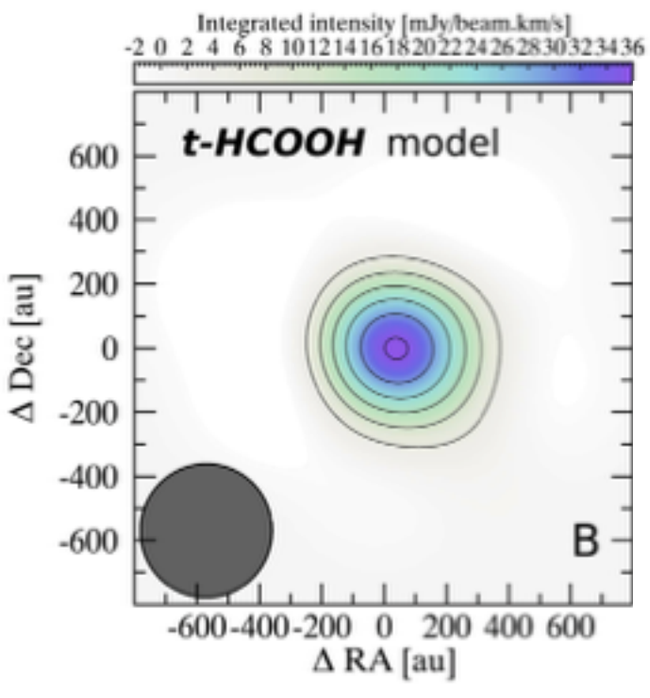

Figure 3. *Panel a*: Observed gas-phase t-HCOOH emission integrated over the line profile after applying a Keplerian mask and smoothed at resolution equivalent to the TW Hya disk size. The contours and level step are at 3σ (where 1σ = 2 mJy beam^{-1} km s^{-1}, in the smoothed and masked data). *Panel b*: Same as *A* but model. The synthesized beam is shown in the bottom left corner of panels A and B.

化学反応を含むモデル計算の疑似観測

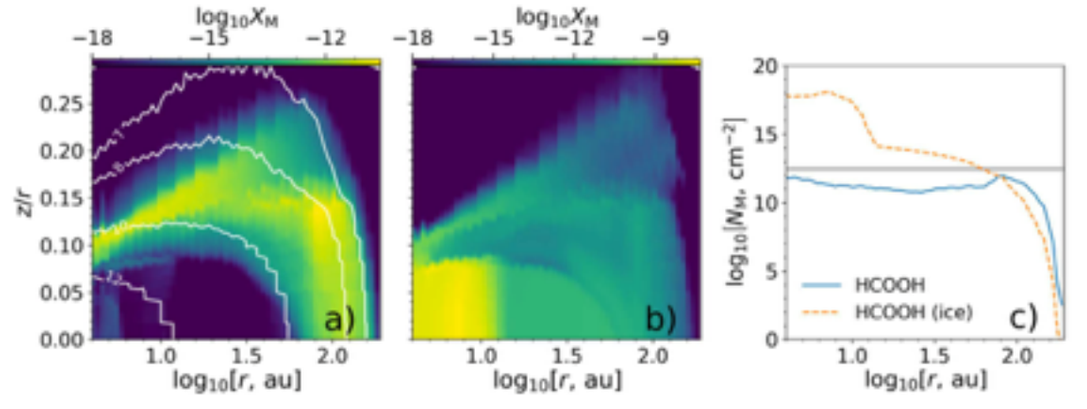

Figure 4. Theoretical t-HCOOH relative abundance to molecular hydrogen. *Panel a*: Spatial distribution of the gas phase abundance as a function of the radial distance from the central star and the altitude over the midplane. The white contours denote log10(n_{H_2}) in cm^{-3}. *Panel b*: Same as A but for the HCOOH ice. *Panel c*: Radial distribution of column densities of gas (blue line) and solid (dashed orange line) HCOOH. The grey line shows the measured HCOOH column density. The predictions are based on our physical and chemical model (Parfenov et al. 2017, see Section 4).

http://arxiv.org/pdf/1807.11860

18

ALMA observations of RCW120 - Fragmentation at 0.01pc scale

Miguel Figueira[1,2], Leonardo Bronfman[2], Annie Zavagno[1], Fabien Louvet[2], Nadia Lo[2], Ricardo Finger[2] and Javier Rodón[3]

- HII領域RCW120の Herschel コア を，ALMA（3mm連続波）で観測し，コアの中に 0.01 pc スケールの小さな分裂構造を発見した.

- 分裂した0.01pcスケールの塊の質量は，分裂前のコアから見積もられるジーンズ質量よりも１桁以上大きかった．乱流や磁場の影響か？

- 分裂塊の一部からCH_3CNやSO_2が観測された．大質量星誕生領域の候補となるだろう.

Herschel cores

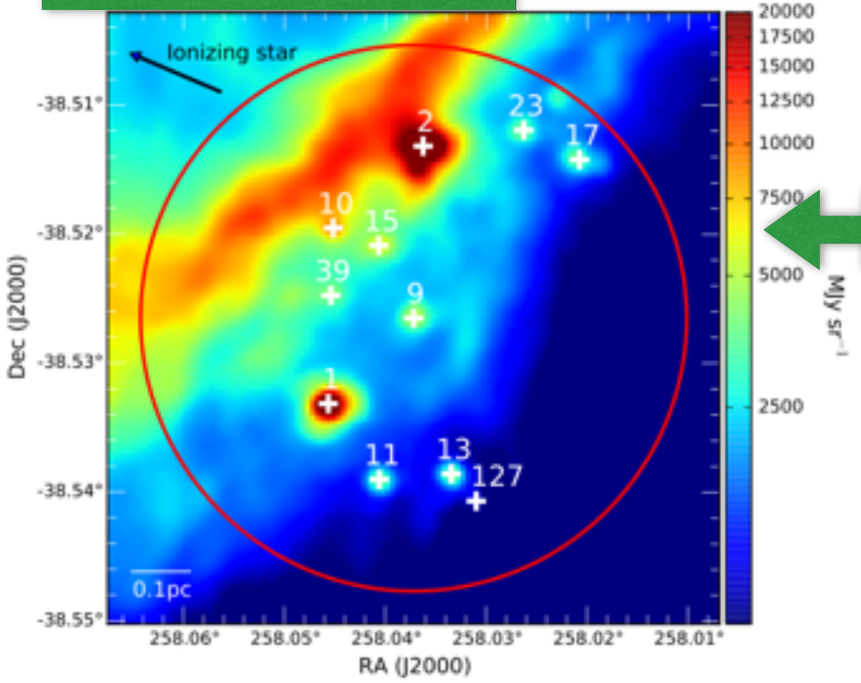

Herschel cores

Id	α J2000 (°)	δ	T_{env} (K)	M_{env} ($M_\odot$)	L_{bol} ($L_\odot$)	n_{H_2}[a] (cm^{-3})	M_{Jeans} ($M_\odot$)	N_{frag}	M_{frag} ($M_\odot$)
1	258.04577	-38.53338	17.0 ± 0.2	85 ± 6	234 ± 28	(3.0±0.2) ×10^5	0.8	2	10.6 ± 0.7
2	258.03624	-38.51317	16.9 ± 0.2	376 ± 21	856 ± 93	(1.3±0.1) ×10^6	0.4	5	73 ± 3.6
9	258.03749	-38.52663	13.1 ± 0.2	97 ± 14	49 ± 12	(3.4±0.5) ×10^5	0.5	2	25.8 ± 1.6
10	258.04524	-38.51956	11.1 ± 0.4	252 ± 41	46 ± 17	(8.7±1.4) ×10^5	0.3	2	15.5 ± 1.4
11	258.04073	-38.53926	14.2 ± 0.4	31 ± 9	24 ± 11	(1.1±0.3) ×10^5	1.1	1	7.4 ± 0.5
13	258.03352	-38.53886	16.3 ± 0.8	8 ± 3	23 ± 9	(2.8±1.0) ×10^4	2.5	2	6.8 ± 0.8
15[b]	258.04084	-38.52110	12.8 ± 0.5	81 ± 15	38 ± 15	(2.8±0.5) ×10^5	0.5	1	3.5 ± 0.6
39	258.04560	-38.52532	12.8 ± 0.3	97 ± 17	42 ± 13	(3.4±0.5) ×10^5	0.5	3	72.2 ± 2.7
17	258.02078	-38.51440	12.8 ± 0.2	122 ± 17	51 ± 13	(4.2±0.6) ×10^5	0.4	0	0
23	258.02648	-38.51204	11.9 ± 0.4	130 ± 21	37 ± 13	(4.5±0.7) ×10^5	0.4	0	0
127	258.03146	-38.54054	10.8 ± 0.3	80 ± 17	12 ± 5	(2.8±0.6) ×10^5	0.4	0	0

Table 1: Properties of the *Herschel* cores using the *getsources* (+*getimages*) algorithm. (1) Identification number, (2,3) J2000 coordinates, (4) Envelope temperature, (5) Envelope mass, (6) Bolometric luminosity, (7) Volume density, (8) Jeans' mass, (9) Number of fragments inside the core, (10) Total mass of the fragments

17, 23, 127番は分裂なし

ALMA 3mm

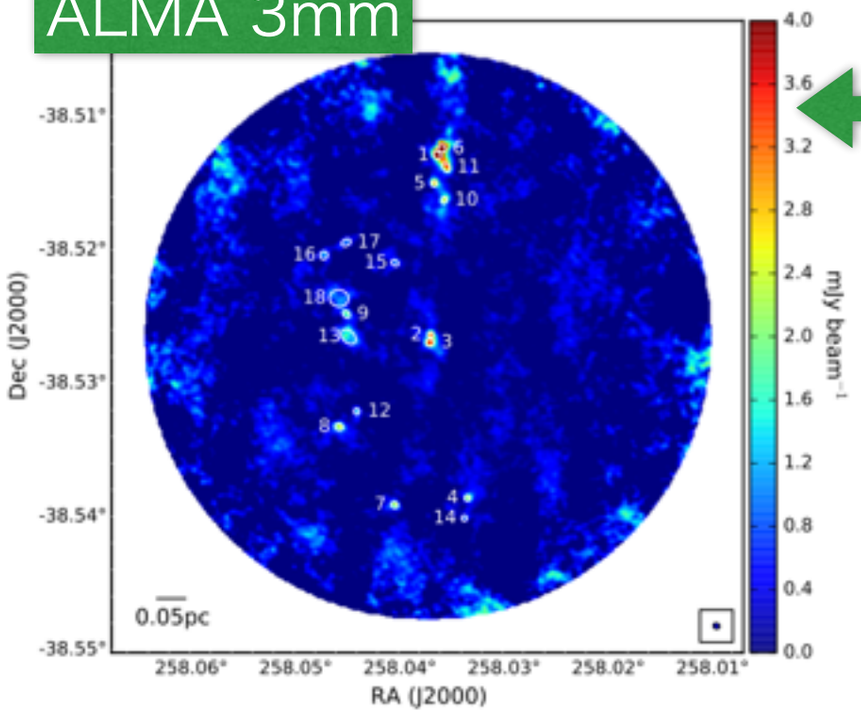

ALMA 3mm

Herschel Core	Id	α J2000 (°)	δ	M_{frag} ($M_\odot$)	Size (mpc)
Core 1	8	258.0457	-38.5333	7.7 ± 0.4	8.7
	12	258.0440	-38.5321	2.8 ± 0.3	3.1
Core 2	1	258.0363	-38.5129	27.4 ± 0.6	8.6
	5	258.0366	-38.5150	5.8 ± 0.6	2.5
	6	258.0358	-38.5124	19.1 ± 1	8.8
	10	258.0356	-38.5163	5.1 ± 0.7	4.3
	11	258.0354	-38.5138	15.7 ± 0.6	10.8
Core 9	2	258.0369	-38.5264	8.2 ± 0.7	1.6
	3	258.0370	-38.5269	17.6 ± 0.9	9.3
Core 10	16	258.0471	-38.5204	7.7 ± 0.8	9.6
	17	258.0450	-38.5194	7.8 ± 0.6	9.9
Core 11	7	258.0404	-38.5391	7.4 ± 0.5	6.9
Core 13	4	258.0334	-38.5386	4.8 ± 0.4	3.1
	14	258.0337	-38.5401	2.1 ± 0.5	10.0[a]
Core 15	15	258.0403	-38.5210	3.5 ± 0.6	6.0
Core 39	9	258.0450	-38.5248	8.7 ± 0.4	8.1
	13	258.0448	-38.5265	31.6 ± 0.7	22.4
	18	258.0457	-38.5236	31.8 ± 1.5	28.8

Table 2: Properties of the fragments detected with ALMA at 3 mm. (1) Fragment's Id, (2,3) J2000-coordinates, (4) Mass assuming the temperature of the hosting core (see Table 1), (5) Deconvolved size

ジーンズ質量よりも，
分裂雲の質量が大きい

乱流を考慮した実行的なジーンズ質量であれば，~100 $M_{太陽}$.

Fig. 1: Top: *Herschel* 70 μm image of Condensation 1 with the sources detected with the *getimages-getsources* algorithms from Figueira et al. (2017), the FoV of the ALMA observation presented here (red circle) and the direction where the ionizing star is located (black arrow). Bottom: 3 mm ALMA image of the fragments observed towards Condensation 1.

ALMA 3mm：Herschel コアの拡大図の例

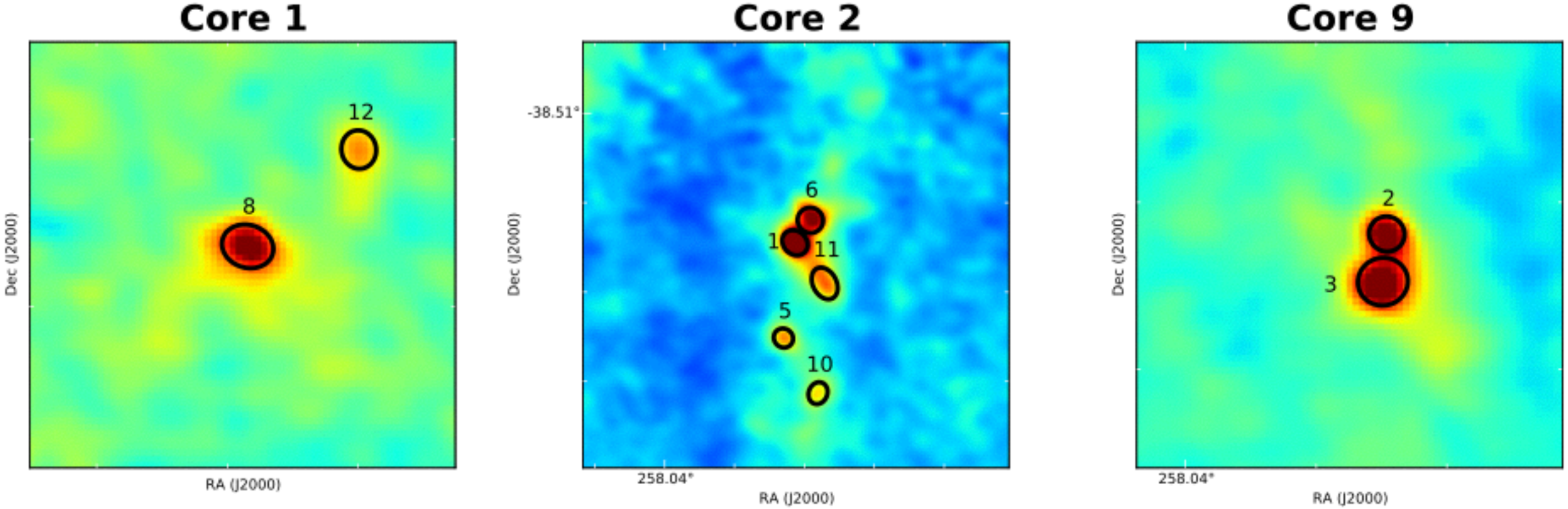

Fig. A.1: ALMA sources extracted with *getsources* (black ellipses) for each of the *Herschel* cores at 3 mm.

ALMA の分子のライン

大質量星形成のトレーサー.

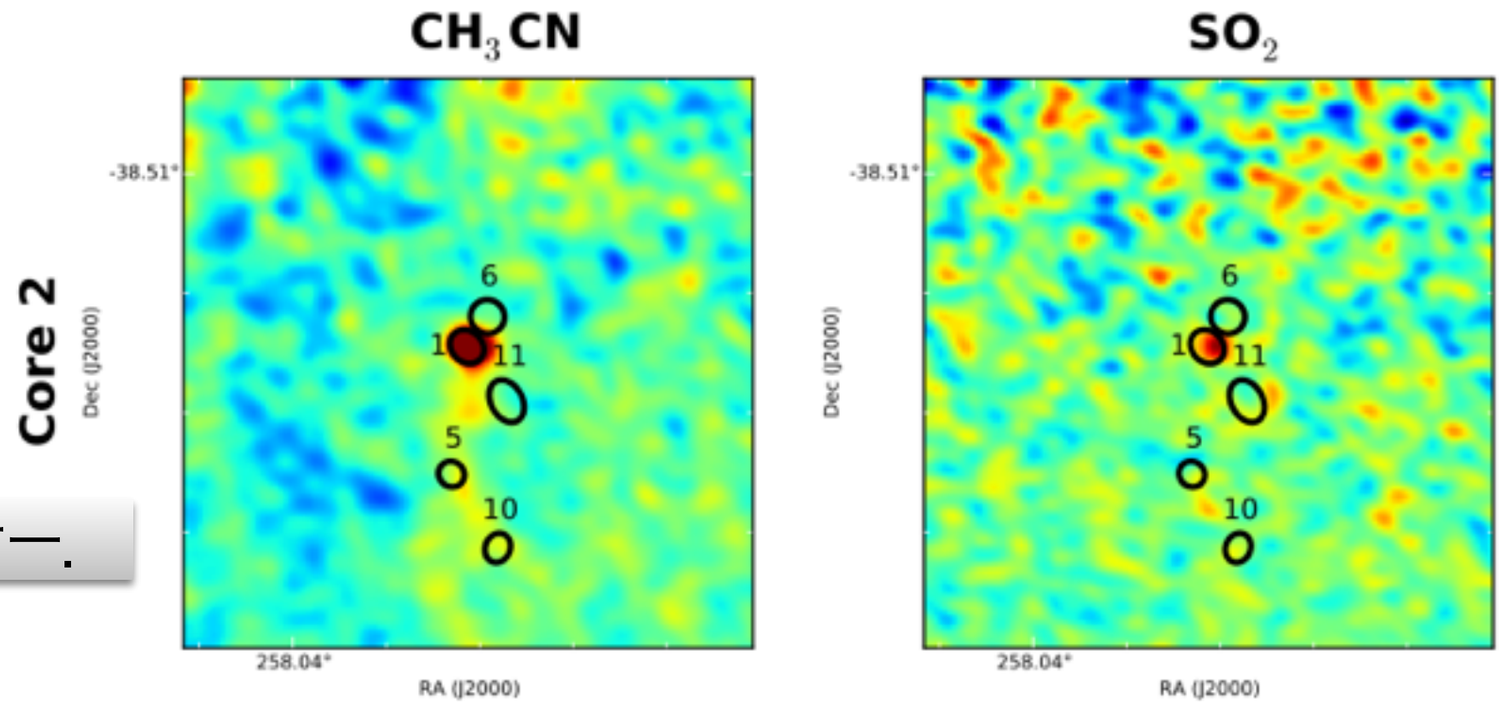

Fig. A.2: Integrated emission of the CH_3CN and SO_2 molcular lines towards the *Herschel* Core 2

http://arxiv.org/pdf/1807.08525

19

A multi-wavelength view of magnetic flaring from PMS stars

E. Flaccomio[1], G. Micela[1], S. Sciortino[1], A.M. Cody[2], M.G. Guarcello[1], M. Morales-Calderón[3], L. Rebull[4], and J.R. Stauffer[4]

- 前主系列星からの磁気フレアの多波長（X線，可視光，中間赤外）での観測データを集めて，時間変化や強度比などを調べた．

- フレアの継続時間が，X線の方が，可視光よりも長い．（太陽フレアのモデルと矛盾がない）

- X線と可視光や中間赤外のエネルギーには相関がある．赤外は星周円盤の有無によって違いがある．

表１：約78個のフレアイベント

発見されたフレアの例

Fig. 2

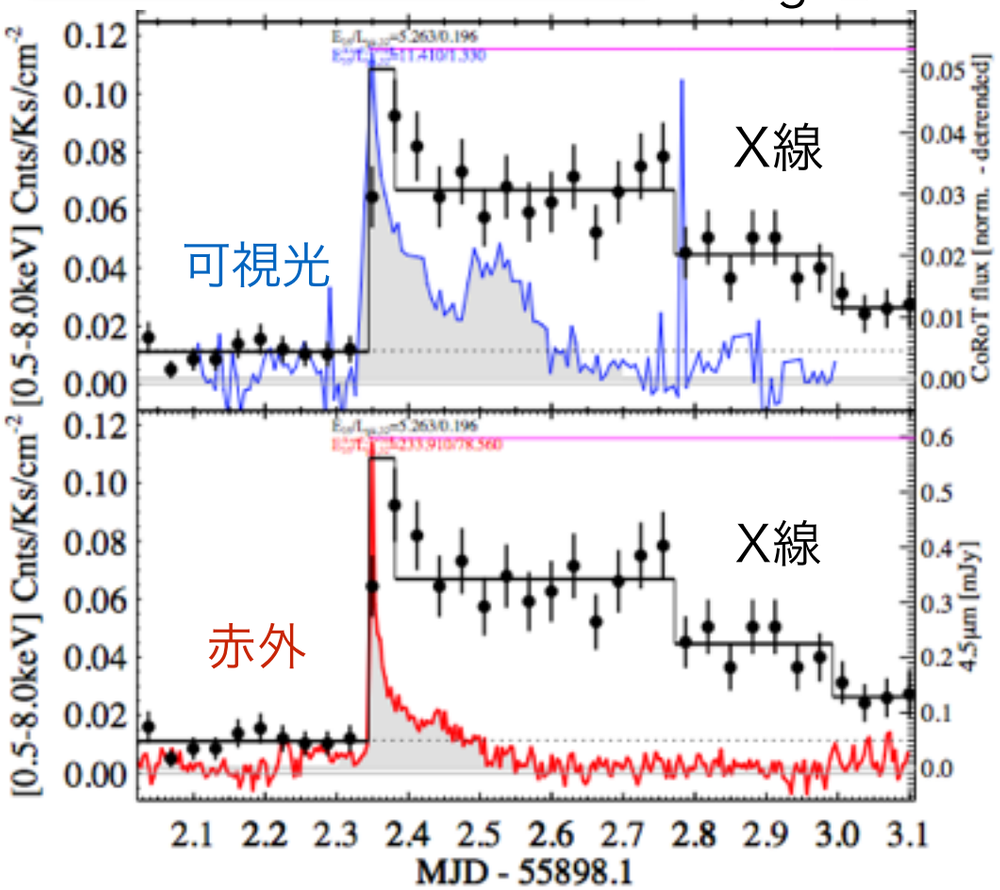

参考

太陽フレア：10^{29}-10^{32} erg

今回のPMSフレア：10^{35}-10^{38} erg

参考：太陽フレアの磁気リコネクションモデル

Shibata et al. 1995, ApJ, 451, p.L83

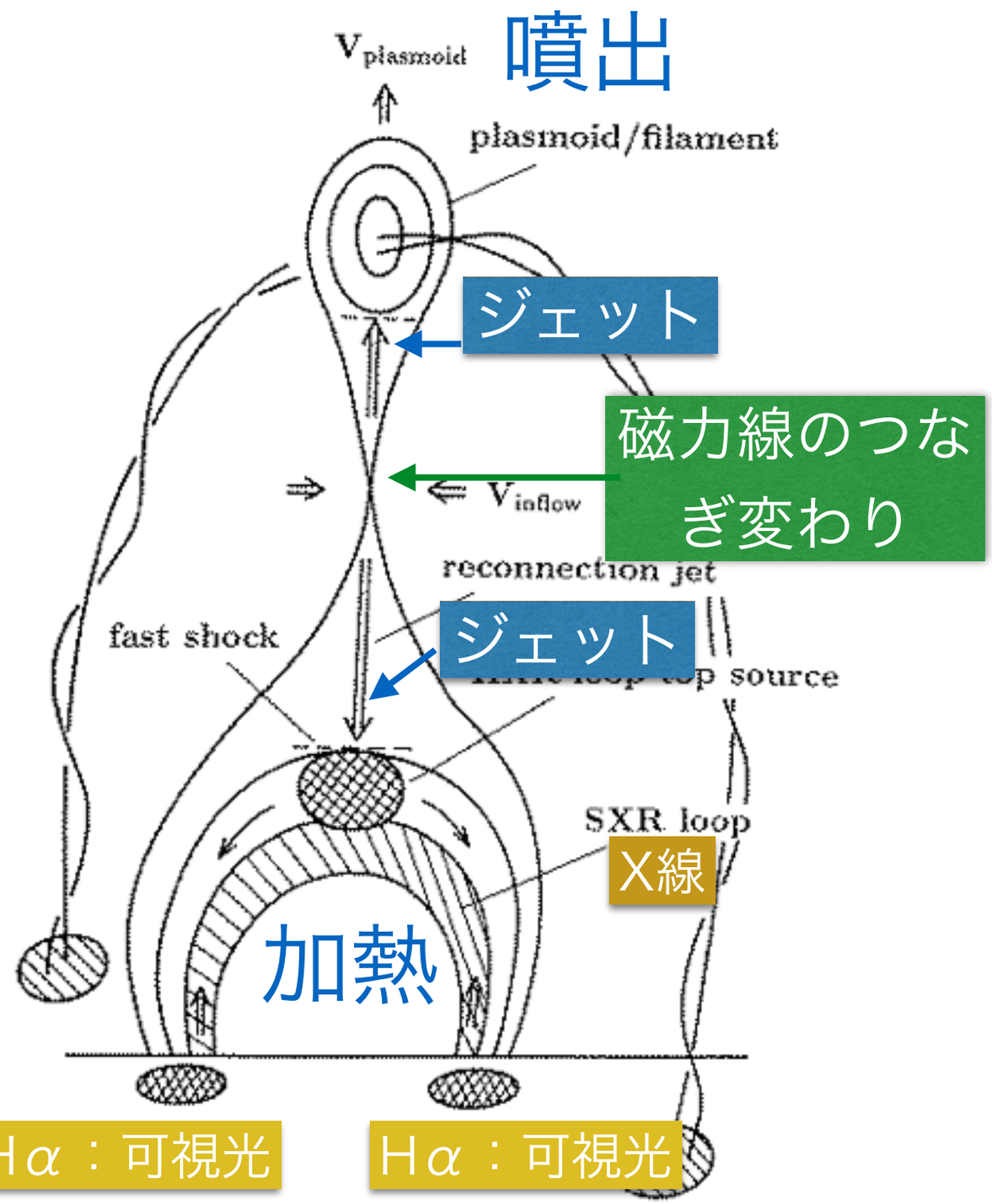

基本的には太陽フレアのモデルと矛盾がなさそう

class III
class II
（白抜きは不確かなデータ）

フレアの発生時刻の差の頻度分布

Fig. 7　　縦軸 頻度,　横軸 発生時刻の差

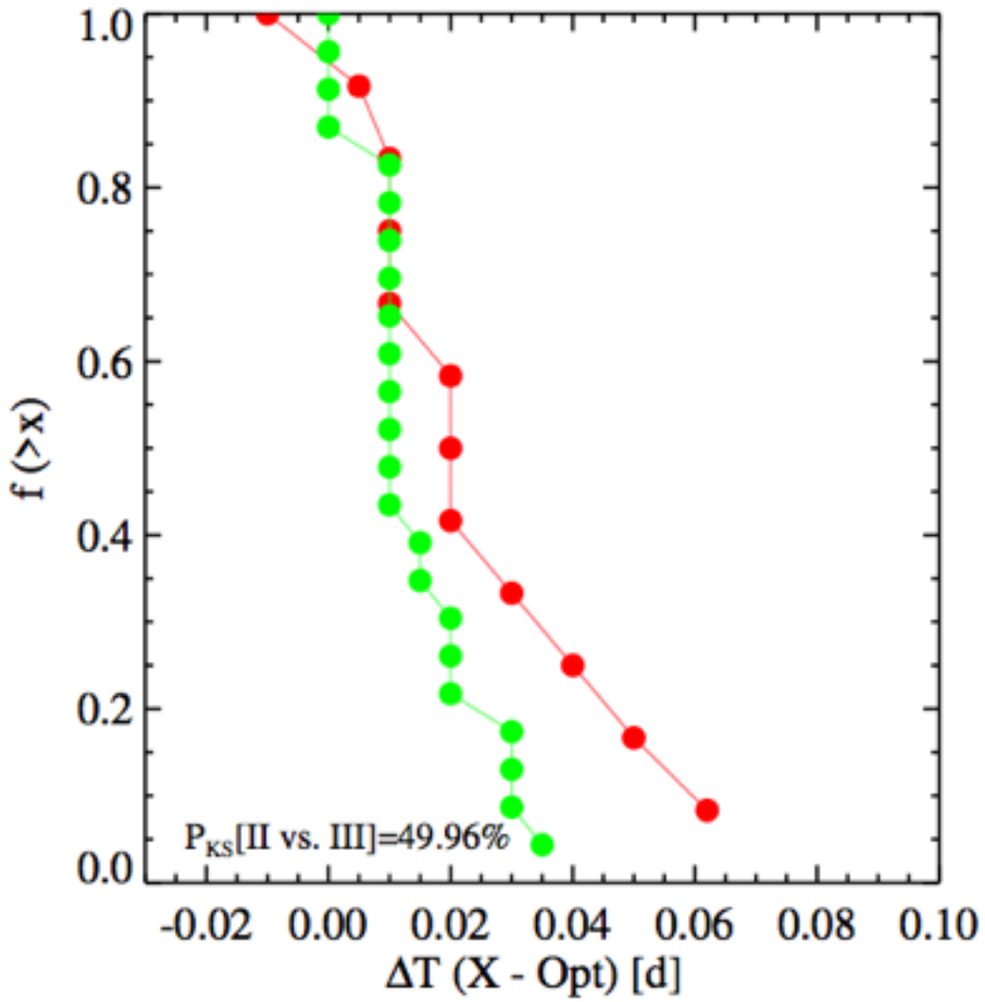

ほぼ同時刻に起こっている

フレアの継続時間

Fig. 6　　縦軸 X線,　横軸 可視光

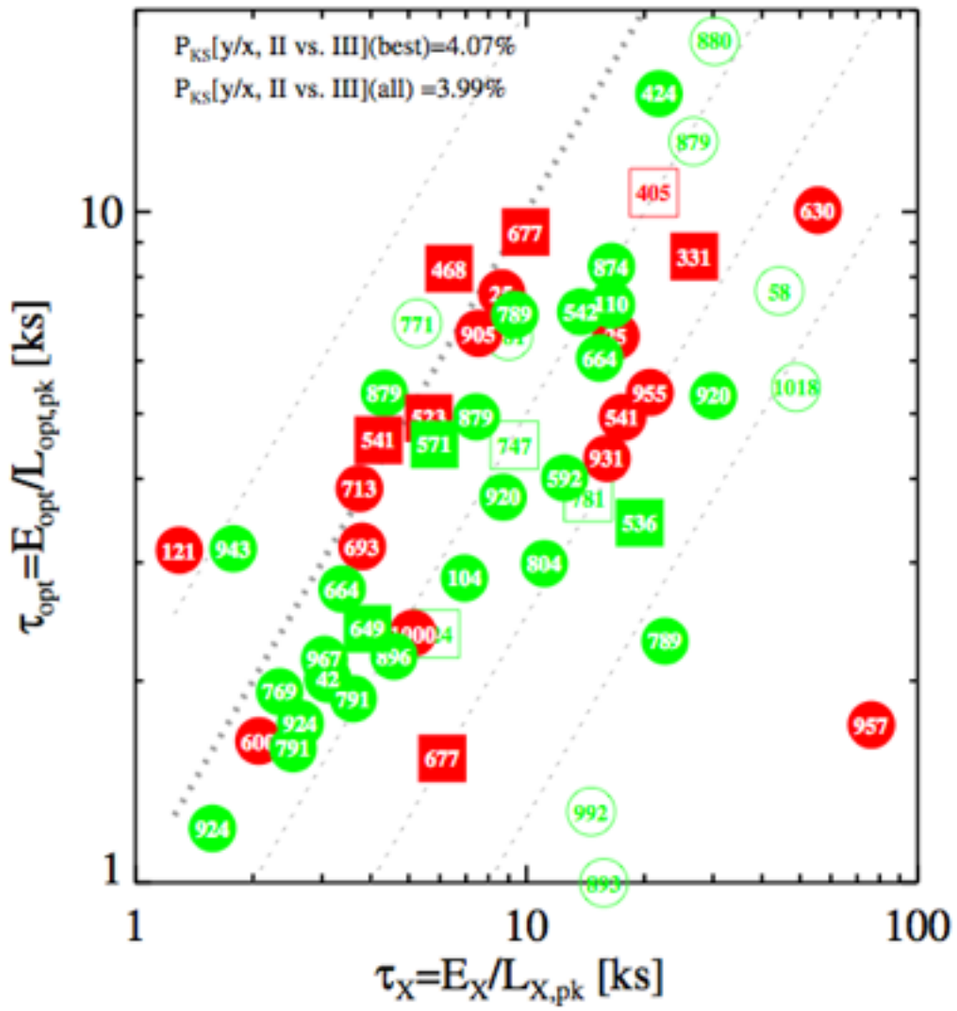

X線の継続時間が,
可視光よりも長い

エネルギーの相関

光から見積もった全エネルギーとXの相関

Fig. 3

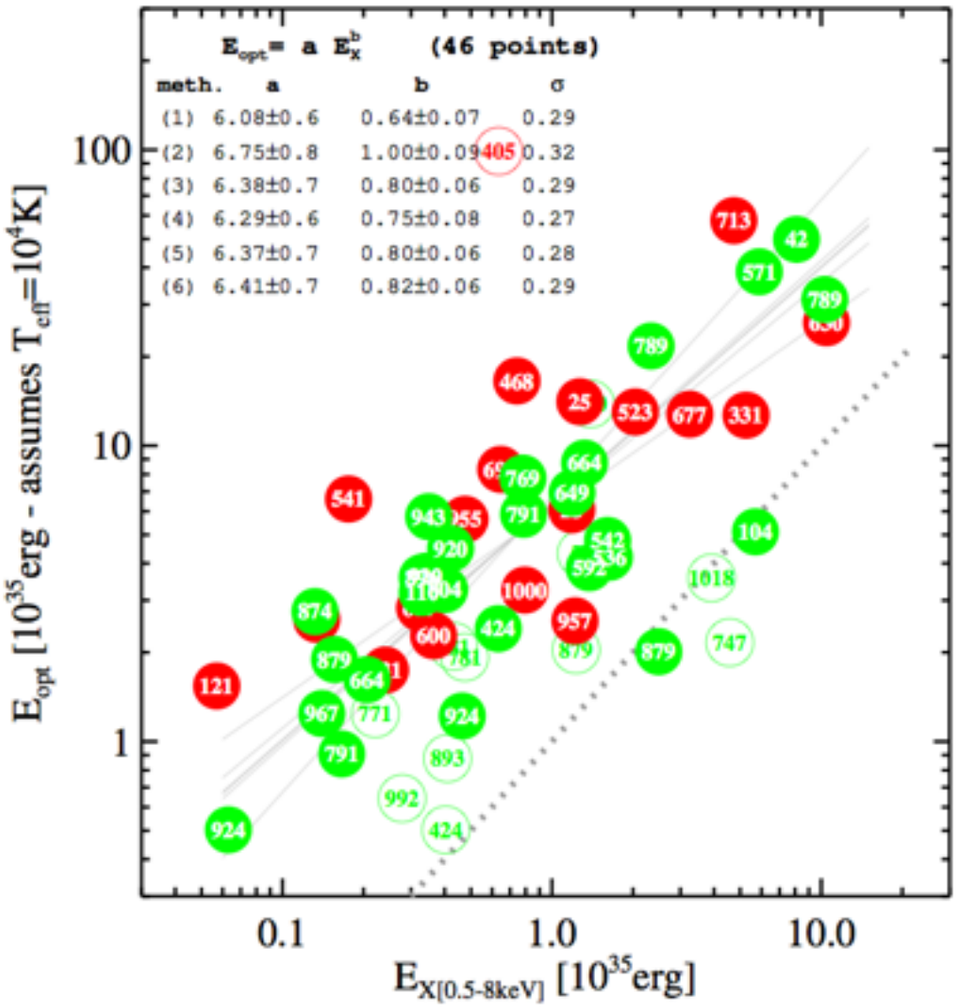

class III

class II　　class I

（白抜きは不確かなデータ）

赤外から見積もった全エネルギーとXの相関

Fig. 4

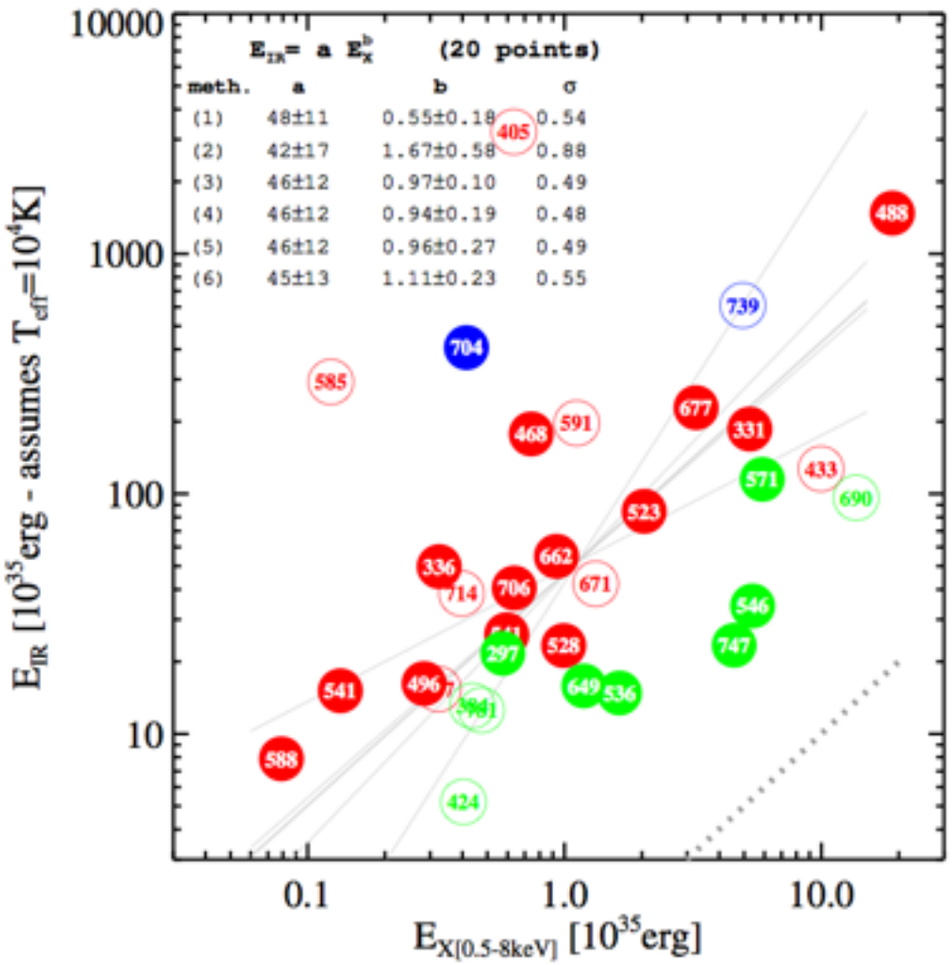

赤外線から見積もると class II は class III よりも明るい.

赤外線は円盤の影響か星周物質の再放射？